ETH zürich

ETH Library

Comparison of swarm and breakdown data in mixtures of nitrogen, carbon dioxide, argon and oxygen

Journal Article

Author(s):
Haefliger, Pascal; Franck, Christian

Publication date:
2019-01-09

Permanent link:
https://doi.org/10.3929/ethz-b-000300734

Rights / license:
Creative Commons Attribution-NonCommercial-NoDerivatives 4.0 International

Originally published in:
Journal of Physics D: Applied Physics 52(2), https://doi.org/10.1088/1361-6463/aae60f

This page was generated automatically upon download from the ETH Zurich Research Collection.
For more information, please consult the Terms of use.

Comparison of swarm and breakdown data in mixtures of nitrogen, carbon dioxide, argon and oxygen

P. Haefliger[1], **C. M. Franck**[1]

[1]Power Systems and High Voltage Laboratories, ETH Zurich, Physikstr. 3, 8092 Zurich, Switzerland

E-mail: `franck@eeh.ee.ethz.ch`

May 2018

Abstract. Mixtures of atmospheric gases such as N_2, CO_2, O_2 and Ar are seen as possible insulation gas in high voltage equipment, both with and without the admixture of a fluorinated gas such as the C_4F_7N nitrile or $C_5F_{10}O$ ketone. Therefore, the binary gas mixtures N_2-O_2, CO_2-O_2, and N_2-CO_2 and some selected ternary gas mixtures were measured with a pulsed Townsend experiment and a breakdown experiment. In order to compare the experimental results, the breakdown voltage was estimated applying the streamer criterion to the effective ionization coefficient obtained with a pulsed Townsend experiment. The comparison shows a very good agreement between the two methods, which implies that it is possible to predict the electrical strength of atmospheric gases in homogeneous electric fields over a wide *pd* range (product of vessel pressure p and electrode gap separation d) from swarm parameters only. Our results show that an admixture of 5% CO_2 to N_2-O_2 mixtures increases the breakdown voltage by 1-2% percent in the measured *pd* range compared to the basis gas mixture. N_2-O_2-CO_2 mixtures with an O_2 concentration between 40-80% and 5% of CO_2 show an increased breakdown strength by around 8% compared to synthetic air (i.e. N_2-O_2 80-20%) without CO_2.

PACS numbers: 00.00, 20.00, 42.10

Submitted to: *J. Phys. D: Appl. Phys.*

1. Introduction

In recent years, industry and academia tried to find a replacement for sulfur hexafluoride SF_6 for the application in high voltage equipment, due to its high global warming potential (GWP). The GWP of SF_6 is given as 23500 relative to CO_2 over a defined period of 100 years [1].
Gases or gas mixtures aiming to reach the same or even higher electrical insulation capability often have other drawbacks such as their long term instability, high boiling point, toxicity or they have a similar GWP as SF_6 [2, 3]. Recently, alternatives such as the C_4F_7N nitrile or $C_5F_{10}O$ ketone, in admixture to CO_2 or CO_2-O_2 mixtures were proposed [4, 5]. Besides this recent development and due to the manifold and complex requirements imposed on replacement gases or mixtures (operating temperature and pressure, stability and toxicity), air-like mixtures (Ar, CO_2, N_2 and O_2, later called "atmospheric gases") are seen by some as a possible replacement in certain applications [2, 6]. The main disadvantage here is that the electric strength is only around one third compared to SF_6. Nevertheless, some publications proposed optimal gas mixtures, aiming for a significant increase in breakdown strength compared to synthetic air [7, 8, 9]. With a systematic and extensive analysis we aim to quantify the possible increase in the insulation performance for binary mixtures of N_2-O_2, CO_2-O_2 and N_2-CO_2 as well as a few ternary mixtures with small admixtures of Ar and CO_2 in N_2-O_2.

To understand to which extent pulsed Townsend experiments can give reliable results for deriving breakdown voltages, these results are compared to experimental breakdown data.

This publication presents details of the pulsed Townsend and breakdown experiment in section 2. In section 3, the methods for data evaluation of both experiments are explained. The results are shown in section 4. In the last part, section 5, we discuss and conclude on the results.

2. Experiment

2.1. Pulsed Townsend experiment

The swarm parameters are obtained using a pulsed Townsend experiment (PT). To summarize the principle in short: A displacement current is caused by electrons and ions moving in a homogeneous electric DC field. This current is amplified with a high bandwidth transimpedance amplifier and recorded by an oscilloscope. The start electrons are provided by the photocathode which is built into the cathode side of the Rogowski shaped electrode system. The photocathode is a quartz window coated with a thin single or double layer metal film. In the presence of oxygen, the number of released electrons decreases drastically with time. The best efficiency and stability were obtained with magnesium-palladium coatings of 15 nm and 5 nm thickness, respectively.

A short UV-laser pulse of about 1.5 ns pulse width (FWHM) and 266 nm wavelength releases a number of electrons in the order of 10^6 to 10^7 from the metal film. To analyze the gas samples, measurements are taken in the pressure range from 2-10 kPa at room temperature. In cases where pressure dependent results are expected, pressures up to 100 kPa were measured. The purity of the used gases is given as 5.0 (99.999%) at least. The experiment details are described in [10, 11], different measurements are attributed accordingly with the acronym PT1 and PT2. The majority of measurements were conducted with PT1, only for the detailed analysis of detachment and ion processes the more accurate PT2 was used [12]. Both setups work by the same principle and are to a high degree automated. In the newer experiment (PT2) the accuracy was improved and examined in detail to an error smaller than ±0.5% in the density-reduced electric field E/N [11].

2.2. Breakdown experiment

The breakdown experiment (Bd) schematics is shown in fig. 1a whereas fig. 1b gives details of the mechanical construction, including the vessel and electrode support system. The HV-circuit is composed of plug and play components from Messwandlerbau Bamberg (MWB). The breakdown experiments are conducted with 50 Hz AC. The setup is limited to a maximum operating voltage of 190 kV and the glass-fiber reinforced epoxy vessel is designed for an absolute pressure of 0.6 MPa and a volume of 11.5 l. The top of the vessel is connected to HV potential and the bottom is grounded via the breakdown detection unit. To limit the energy of the arc during breakdown, equal sized 50 kΩ resistors R1 and R2 are included in the high-voltage (HV) circuit. Additionally, the discharge duration is limited by a breakdown detection (det) feedback loop, turning off the HV-Source (U) after 20 to 30 ms. A capacitive divider (C=50 pF) and a measurement unit of the brand MU17 HIGHVOLT are used to measure the voltage (AC peak voltage). The estimated overall voltage measurement error is 2%. The pressure sensor, as well as the gas in- and outlet pipes are connected via boreholes on the bottom. The gas inlet is connected to a panel where up to four gases can be mixed. The pressure and temperature is measured with a WIKA pressure sensor of type CPG1500 which has an accuracy of 0.1% full scale with a range from 0 to 0.6 MPa.

Two stainless steel (1.4460) electrodes with Rogowski shaped profile are used to obtain a homogeneous electric field. The electrode diameter is 80 mm with a flat area of 40 mm diameter. The electrode profile is optimal for a 15 mm electrode gap distance. A separate inner polyethylene electrode-support tube guarantees a pressure independent positioning of the electrodes. The electrodes parallelism is fine tuned with adjustment screws to ±5 μm, and determined with gage blocks (resolution of 1 μm). The overall electrode gap separation, on the other hand, is subject to temperature effects and accurate to ±80 μm. To avoid a lack of start electrons the electrode surface is regularly sandblasted. The measured surface roughness R_a (arithmetic average) and R_t (maximum height of the

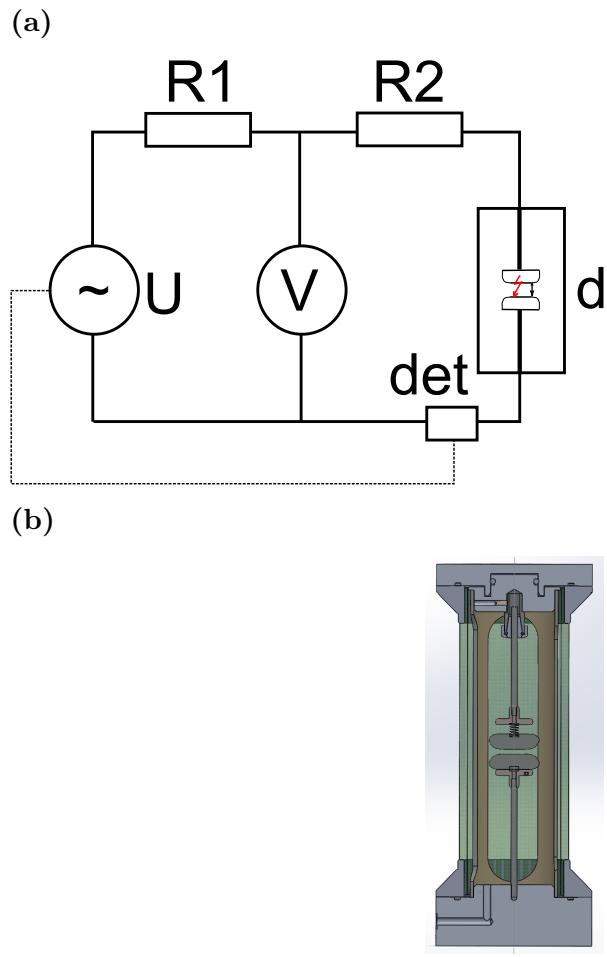

Figure 1: **a)** Schematics of breakdown circuit. U controlled 50 Hz AC voltage source (including a HV transformer), R1, R2 current limiting resistors, V voltage measurement, det breakdown detection unit with feedback to voltage source and the test vessel with electrodes at gap distance d. **b)** Schematic of breakdown chamber with Rogowski profile shaped steel electrodes.

profile) is around 2-4 μm and 13 μm. The homogeneous electric field distribution and good parallelism is confirmed after the experiments as the visible breakdown marks are well distributed over the whole electrode surface.

Before filling the gas sample into the experimental vessel, the vessel is evacuated down to a base pressure of 50 Pa. Subsequently, the gases are slowly (the filling procedure takes about 30 minutes) filled to pressures of up to 0.5 MPa. A breakdown measurement series at fixed pressure consists of 250 breakdowns, which are obtained from rising voltage tests. The chosen rate of rise depends on the absolute magnitude of the expected breakdown voltage U_{Bd}, and lies in the range of 0.1 to 0.2 kV/s. Between subsequent breakdowns, the elapsed time is 3 minutes. In order to control humidity, water absorbing silica gel bags are placed inside the chamber. Without these gel bags, increasing humidity over time was measured, which leads to a noticeable increasing trend in U_{Bd} over time.

The measurement results may be influenced by many parameters such as waiting time between breakdowns, reduction of pressure for subsequent measurements, voltage rising rate, gas humidity and lack of start electrons. The U_{Bd} results were statistically tested and mentioned values were kept constant as listed, to enable constant conditions for breakdowns and to realize a low, not significant influence on final breakdown results.

3. Evaluation method

In the framework of this report, three different approaches are followed to determine the breakdown voltage in homogeneous gaps

a) via $(E/N)_{\mathrm{crit}}$ PT
b) via the streamer criterion PT
c) via the direct breakdown voltage measurement Bd

3.1. Pulsed Townsend experiment

The measured displacement current is the superposition of electron and (positive and negative) ion current. The evaluation routine is based on [10] and [13]. The used electron current model equation $I_e(t)$ describes the electron component with an analytical formula eq. (1). T_0 is the instant the electrons are released from the photocathode. The initial current amplitude is I_0, n_0 is the number of electrons with elementary charge q_0. T_{e} is the electron drift time which relates to the electron bulk velocity via $w_{\mathrm{e}} = d/\ T_{\mathrm{e}}$, where d is the electrode gap distance. During the electron drift the electron number changes exponentially with the effective ionization rate ν_{eff} and the swarm broadens with the characteristic time for longitudinal diffusion τ_{D}. The measured current and hence the resulting swarm parameters depend on E/N which is the applied electric field E and the gas number density N.

$$I_{\mathrm{e}}(t) = \frac{I_0}{2} \exp\left(\nu_{\mathrm{eff}}(t - T_0)\right) \left(1 - \mathrm{erf}\left(\frac{t - T_{\mathrm{e}}}{\sqrt{2\tau_{\mathrm{D}}(t - T_0)}}\right)\right) \tag{1}$$

$$I_0 = \frac{n_0 q_0}{(T_{\mathrm{e}} - T_0)} \tag{2}$$

The longitudinal diffusion coefficient D_{L} and effective ionization coefficient α_{eff} can be obtained using the following relations:

$$2D_{\mathrm{L}} = \tau_{\mathrm{d}} \cdot w_{\mathrm{e}}^2 \tag{3}$$

$$\alpha_{\mathrm{eff}} = \nu_{\mathrm{eff}}/w_{\mathrm{e}} \tag{4}$$

The model was extended in [13] to separate ν_{eff} into the contributions of attachment ν_{a} and ionization ν_{i} and further the ion drift velocities, w_{p} for positive and w_{n} for negative ions were obtained. If more gas kinetics such as detachment processes and ion conversion occur, other evaluation methods are applied [12, 14].

3.2. Critical electrical field strength

Electron attaching gases remove free electrons in the gas and form negative ions. The critical field strength $(E/N)_{\text{crit}}$ is defined as, the E/N value where attachment equals ionization and hence the effective ionization rate is zero, $\nu_{\text{eff}} = \nu_{\text{i}} - \nu_{\text{a}} = 0$. An U_{crit} critical voltage can be calculated according to eq. 5.

$$U_{\text{crit}} = (E/N)_{\text{crit}} \cdot Nd. \tag{5}$$

3.3. Streamer criterion

A known method to link swarm results (effective ionization coefficient α_{eff}) to breakdown voltages is the streamer criterion in eq. (6). In general, the α_{eff} is integrated along the electric field line, up to the boundary x_c where $(E/N)_{\text{crit}}$ is reached. The breakdown criterion is fulfilled if the integral is equal or larger than the streamer constant K.

$$\int_0^{\text{x}_\text{c}} \alpha_{\text{eff}} \, \text{d}x \geq K \tag{6}$$

In homogeneous electric fields the relation simplifies to

$$\frac{\alpha_{\text{eff}}}{N} = \frac{K}{Nd}. \tag{7}$$

A reasonable value for K is K=12 [15]. This value fits best when comparing our results to reference data. The sensitivity of U_{Bd} to the value K is discussed in section 4.5.

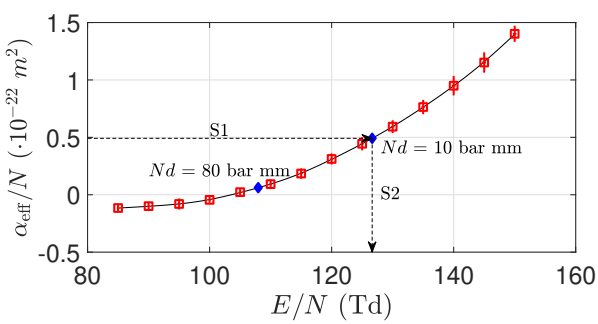

Figure 2: (□) α_{eff}/N for N_2-O_2 79-21% mix [16], (——) spline fit of α_{eff}/N. (♦) specific values of the ratio (K/Nd). S1, S2 are step 1 and 2 of the graphical interpretation to calculate the breakdown voltage using the streamer criterion for homogeneous electric fields.

The homogeneous field breakdown voltage is calculated in two steps with eq. (7) and

$$U_{Bd}^{calc} = \frac{E}{N}\left(\alpha_{\text{eff}} = \frac{K}{Nd}\right) \cdot Nd. \tag{8}$$

First, the $K/(Nd)$-value on the plotted α_{eff}/N curve (S1) must be found and in the second step the corresponding E/N value (S2) is determined, which we define as the calculated breakdown field strength $(E/N)_{\text{Bd}}^{\text{calc}}$. $(E/N)_{\text{Bd}}^{\text{calc}}$ multiplied by Nd gives the calculated breakdown voltage $U_{\text{Bd}}^{\text{calc}}$, eq. (8). These steps are shown in fig. 2 for the effective ionization coefficient of air at 10 bar mm.

3.4. Breakdown experiment

Breakdowns are forced by steady increase of the applied AC voltage at the electrode gap. The breakdown process is of statistical nature and the measured breakdown voltages varies slightly. It is evaluated with well-known statistical methods [17].
It was taken care of that subsequent breakdowns are independent of the previous ones and which was checked with iteration tests. If measurement series showed a dominate trend over time, the cause was identified and the measurement repeated under improved conditions.

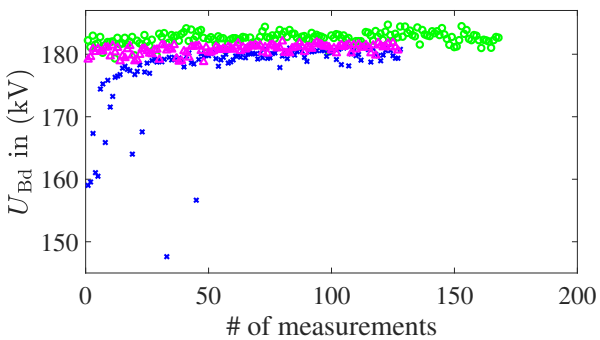

Figure 3: Breakdown measurements performed at the setup's highest possible *pd* values (70 bar mm) in a N_2-O_2 80-20% mixture for different electrode conditions. (x) newly sandblasted electrode, electrode surface conditioning visible, (△) regular measurement series after conditioning with 250 shots, (o) excessively stressed electrode after 4500 breakdowns, with slightly different electrode spacing.

According to Paschen's law, the breakdown voltage U_{Bd} is a function of *pd* alone, i.e. the product of pressure and electrode gap distance. Hence, breakdown measurements were performed for different *pd*. The chosen unit is bar mm which is a widely used unit in publications. To convert p into N, a $T = 293\,\mathrm{K}$ is used. In our setup the maximum pd for atmospheric gas mixtures is 70 bar mm. Example measurements for N2-O2 80-20%, *pd*= 70 bar mm (15 mm 4.66 bar) are shown in fig. 3. Measured U_{Bd} values are normalized to a certain pressure p, temperature T and distance d to make the U_{Bd} of slightly different experimental conditions comparable. T is always normalized to 293 K. Sandblasting is a regularly repeated procedure to provide start electrons. The micro tips building the rough surface emit start electrons via electric field emission process. Over time, with an increasing number of breakdowns, the rough surface is smoothed and therefore the procedure of sandblasting needs to be repeated. Initially after sandblasting, conditioning effects occur, which are shown in the (x) measurement. As is clearly visible in fig. 3 is that some breakdowns for (x) have a U_{Bd} significantly lower than the expected values which is attributed to the effect of electrode surface conditioning. After 250 breakdowns, the conditioning phase has ended and regular measurements as shown with (△) are recorded. After 2500 breakdowns the sandblasting and conditioning procedure

is repeated. (o) measurement series is taken after 4500 breakdowns and the lack of start electrons starts to dominate the measurement, therefore the measured U_{Bd} tends to higher values. Therefore, measurement (x) and (o) represent extreme conditions which are avoided for normal measurement series.

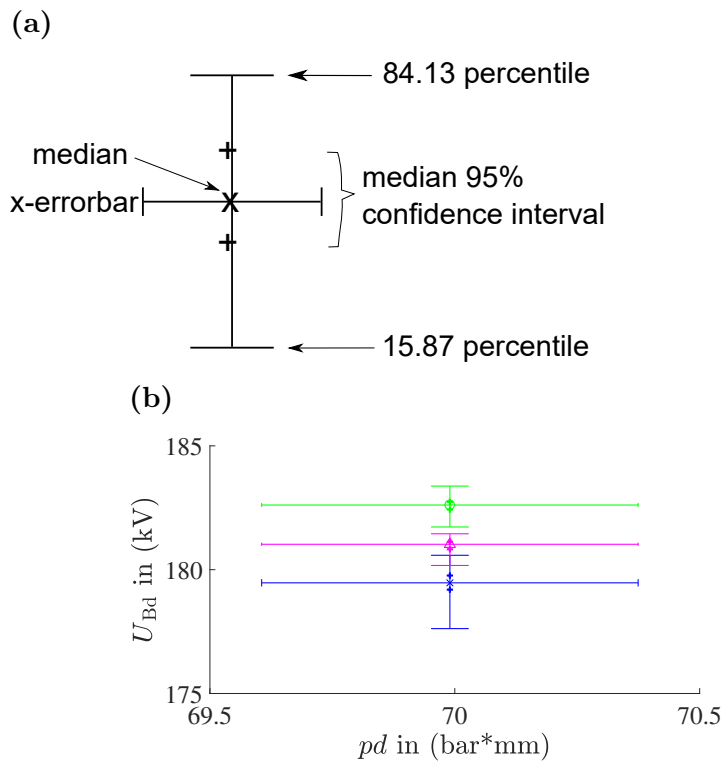

Figure 4: **a)** Representation of a breakdown measurement series of usually more than 200 shots, with (x) median value, (+) median 95% confidence interval and 84.13 and 15.87 percentile as error bars. **b)** Median, median 95% confidence interval and 84.13 and 15.87 percentile plotted for data presented in fig. 3. Symbols and color code are identical.

In the breakdown result plots, the median value is chosen [18] as measured breakdown voltage $U_{\mathrm{Bd}}^{\mathrm{meas}}$ which is shown in fig. 4a. Around the median an upper and lower (+) marks the 95% confidence interval of the median. The median confidence interval represents the quality and number of performed breakdown measurements. The upper and lower error bars give the 84.13 and 15.87 percentile, which are equal to $\pm\sigma$ if the data is normal distributed. In fig. 4b this method was applied to the data from fig. 3. When $U_{\mathrm{Bd}}^{\mathrm{meas}}$ is scaled with Nd the reduced measured breakdown field $(E/N)_{\mathrm{Bd}}^{\mathrm{meas}}$ is obtained.

4. Results

4.1. Overview of the measurements

During the course of analyzing atmospheric gases swarm results for Ar-O_2 were published at POSMOL [19] and N_2-O_2 results were published at Cigre [16]. In this publication swarm measurements of CO_2-O_2 and N_2-CO_2 mixtures are shown. These measurements were conducted with the experiment presented in [10]. All data was analyzed with the method presented in [13]. The results are either obtained from individual pressures and labeled or the average of several pressures (2, 3, 5 and 8 kPa). Similar swarm measurements for N_2-CO_2 and CO_2-O_2 mixtures were published by [20]. N_2-O_2 mixture measurements at elevated pressures of above 10 kPa show significant influence of detachment and ion conversion processes [21, 22]. To obtain conclusive results, these measurements demand a high accuracy. Therefore, measurements were repeated with the experiment explained in [11] and discussed in detail in [14]. Still, it is not fully clear how small admixtures of Ar or CO_2 influence the breakdown strength of air and oxygen and how accurate used swarm results predict breakdown results of these mixtures. The air + CO_2 and Ar mixtures are investigated using the setup [11] and the evaluation method [13] where α_{eff} for pressures above 20 kPa was obtained using w_{e} from 3 kPa measurements. For these mixtures pressures up to 100 kPa in 20 kPa pressure steps were measured. All swarm data will be uploaded to LXCat in the section [23]. A summary of the swarm measurements is given in table 1.

Breakdown measurements were performed for the same gas mixtures as the swarm experiments with the exception of additional breakdown measurements for mixtures of CO_2-O_2-5-95% and N_2-O_2-CO_2-35-60-5%.

4.2. Swarm parameters of N_2-CO_2 *and* CO_2-O_2 *mixtures*

In fig. 5 the effective ionization rate coefficient ν_{eff}/N, electron drift velocity w_{e} and longitudinal diffusion coefficient ND_{L} of N_2-CO_2 mixtures are plotted. In fig. 5a) ν_{eff}/N is shown, CO_2 attaches electrons which leads to the result that mixtures with higher CO_2 concentration have a smaller ν_{eff}/N for low E/N values. After the zero crossing of ν_{eff}/N, ν_{eff}/N increases with increasing CO_2 content. The zero crossing of the rates is not sorted by increasing CO_2 concentration and a slight maximum could be possible in $(E/N)_{\text{crit}}$. However, the E/N resolution of the measurements with 5 Td is too coarse to give a clear answer to this small effect. The results are compared to Magboltz [24] and Bolsig+ [25] calculations. The used cross sections are the embedded cross sections from version 10.2 in Magboltz and the SIGLO cross section set [26] from 2011 for Bolsig+. Our results agree better with Magboltz which we attribute to the input cross section set rather than the calculation method as already pointed out in [11]. The electron drift velocity in fig. 5b) and longitudinal diffusion coefficient in fig. 5c) increase with increasing CO_2 concentration. The electron drift velocity is in good agreement

component	ratio (%)	pressure (kPa)	experiment	publication
Ar-O_2	99-1, 98-2, 96-4, 92-8, 75-25, 50-50, 25-75	2, 3, 5, 8,	PT1 [10]	[19]
N_2-O_2	98-2, 95-5, 92-8, 84-16, 79-21, 60-40, 40-60, 20-80	2, 3, 5, 8, 10.5	PT1 [10]	[16]
CO_2-O_2	95-5, 80-20, 60-40, 50-50, 40-60, 20-80	2, 3, 5, 8, 10.5	PT1 [10]	
N_2-CO_2	95-5, 80-20, 60-40, 50-50, 40-60, 20-80	2, 3, 5, 8, 10.5	PT1 [10]	
N_2-O_2	80-20	3, 6, 10, 20, 40, 60, 80, 100	PT2 [11]	[14]
N_2-O_2-CO_2	75-20-5	3, 6, 10, 20, 40, 60, 80, 100	PT2 [11]	
N_2-O_2-CO_2	55-40-5	3, 4, 5, 6, 8	PT1 [10]	
N_2-O_2-Ar	75-20-5	3, 6, 10, 20, 40, 60, 80, 100	PT2 [11]	

Table 1: Overview of the investigated atmospheric gas mixtures.

to Bolsig+ and Magboltz whereas ND_{L} follows the trend of Magboltz but at a higher magnitude for increasing CO_2 concentration.
In fig. 6 the ν_{eff}/N and w_{e} of CO_2-O_2 mixtures are shown. In fig. 6a ν_{eff}/N is decreasing with increasing O_2 concentration due to attachment. Measurements are in reasonable agreement to Bolsig+ and Magboltz calculations, but fit better to Magboltz results overall. In fig. 6b it seems that O_2 has a lower drift velocity than CO_2 at low E/N but a higher drift velocity than CO_2 at high E/N therefore, the velocities of the different mixtures cross at a certain E/N-value.

4.3. $(E/N)_{\mathrm{crit}}$ *of* N_2-O_2, CO_2-O_2, N_2-CO_2 *and Ar*-O_2 *mixtures*

The density-reduced critical electric field $(E/N)_{\mathrm{crit}}$ derived from swarm experiments as a function of the mixing ratio is shown for N_2-CO_2 and CO_2-O_2 mixtures in fig. 7. For comparison N_2-O_2 [16] and Ar-O_2 mixtures [19] are added. For mixtures with very low attachment rates, we were not able to detect a $(E/N)_{\mathrm{crit}}$ for N_2-CO_2 mixtures below a concentration of 40% CO_2. The $(E/N)_{\mathrm{crit}}$ values for N_2-CO_2 mixtures with higher CO_2 concentrations stay around the $(E/N)_{\mathrm{crit}}$ of pure CO_2. Looking at CO_2-O_2 mixtures, they increase from $(E/N)_{\mathrm{crit}}$ of CO_2 to O_2. Comparing CO_2-O_2 to N_2-O_2 mixtures, the synergy effect of CO_2 with O_2 is smaller than for N_2.
Previous measurements and results as published in [16] suffered from problems with determining the electrode gap distance d accurately. This matter is resolved with [13] and lead to small changes in the swarm results. Accordingly, the newer results show a

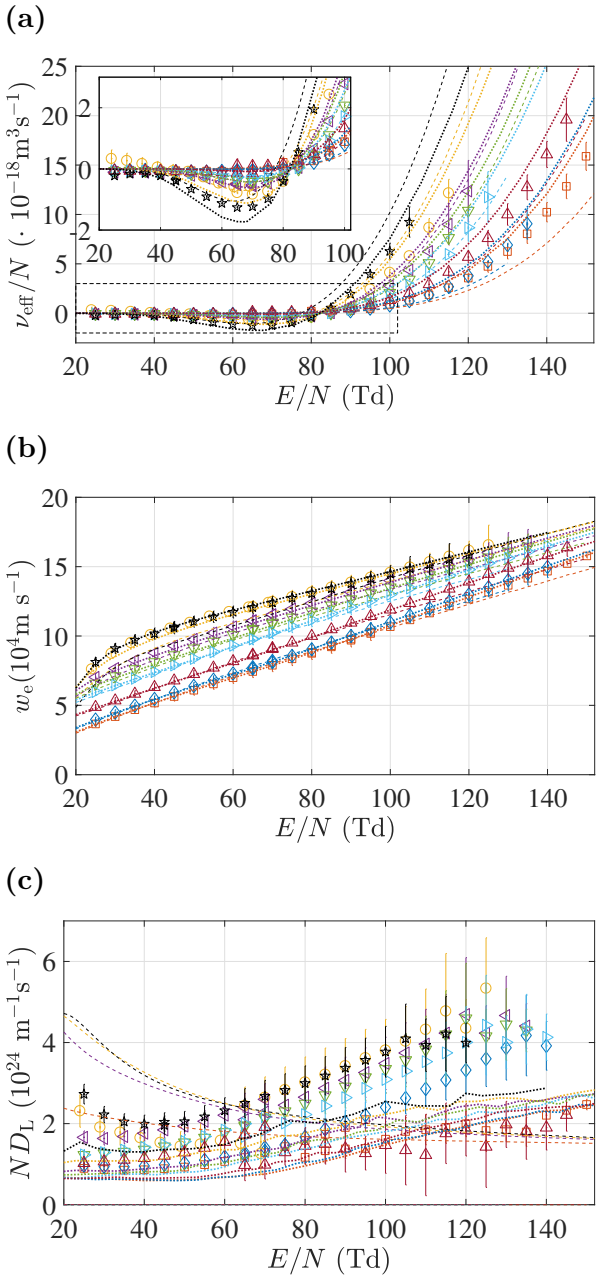

Figure 5: The swarm parameters of the different N_2-CO_2 mixtures are color-coded and indicated by using different symbols: (□) N_2-100%, (◇) N_2-CO_2-95-5%, (△) N_2-CO_2-80-20%, (▷) N_2-CO_2-60-40%, (▽) N_2-CO_2-50-50%, (◁) N_2-CO_2-40-60%, (○) N_2-CO_2-20-80%, (⋆) CO_2-100%. The color-coded lines represent (·····) Magboltz [24] and (- - - -) Bolsig+ [25] calculations. **a)** Effective ionization rate coefficient $\nu_{\rm eff}/N$. **b)** Electron drift velocity $w_{\rm e}$. **c)** Longitudinal diffusion coefficient $ND_{\rm L}$.

small shift in $(E/N)_{\rm crit}$ and a slight optimum in $(E/N)_{\rm crit}$ for N_2-O_2 mixtures around a concentration of 60-80% of O_2 (see zoom in inset of fig. 7). By contrast, in [16] the values for pure O_2 had the highest $(E/N)_{\rm crit}$.

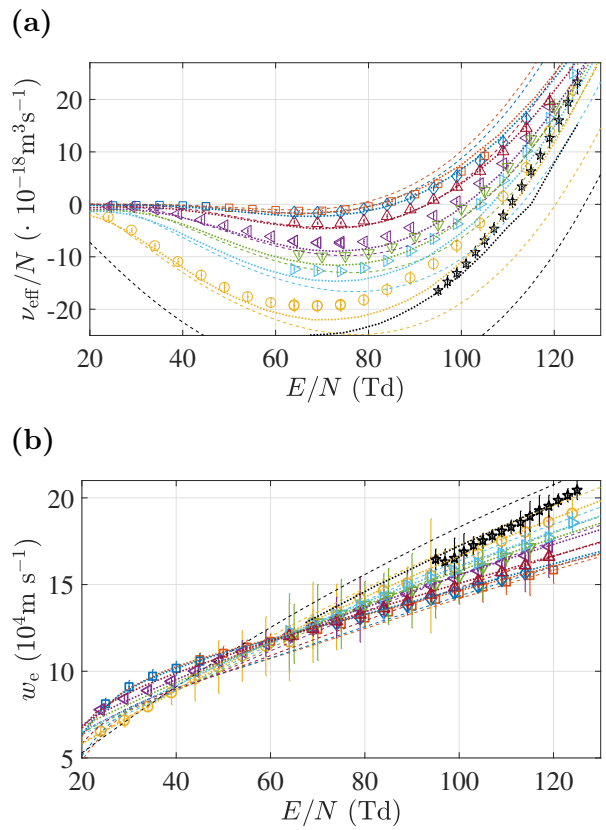

Figure 6: The swarm parameters of the different CO_2-O_2 mixtures are color-coded and indicated by using different symbols: (□) CO_2-100%, (◇) CO_2-O_2-95-5%, (△) CO_2-O_2-80-20%, (▷) CO_2-O_2-60-40%, (▽) CO_2-O_2-50-50%, (◁) CO_2-O_2-40-60%, (○) CO_2-O_2-20-80%, (⋆) O_2-100%. The color-coded lines represent (·····) Magboltz [24] and (- - - -) Bolsig+ [25]. **a)** Effective ionization rate coefficient $\nu_{\rm eff}/N$. **b)** Electron drift velocity $w_{\rm e}$.

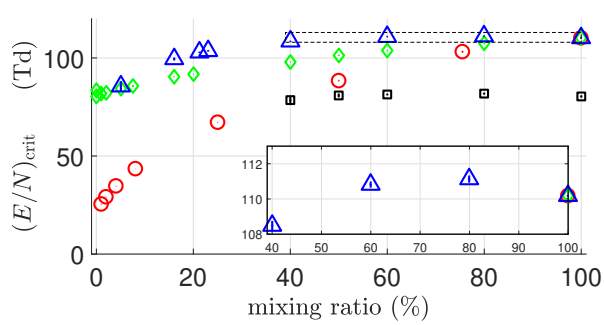

Figure 7: Density-reduced critical electric field $(E/N)_{\rm crit}$ for different mixing ratios of (△) N_2-O_2 [16], (◇) CO_2-O_2, (□) N_2-CO_2 and (○) Ar-O_2 [19] mixtures.

4.4. Swarm measurements of N_2-O_2 *and Ar or* CO_2 *admixtures*

Admixtures of Ar or CO_2 to N_2-O_2 mixtures, and especially to N_2-O_2-80-20%, are of great interest for high voltage insulation. Several studies [9, 7] found that the electric

strength of such mixtures is significantly increased compared to air only. In the following, swarm measurements in these mixtures are presented in detail.

Mixtures of N_2-O_2-80-20%, N_2-O_2-Ar-75-20-5% and N_2-O_2-CO_2-75-20-5% show nearly no difference in the measured displacement current at low pressures like 6 kPa, as depicted in fig. 8a. For simplicity, these mixtures will be denoted as air, air + CO_2 and air + Ar in the following. Yet, the displacement currents start to differ at higher pressures as shown in fig. 8b on the example of 60 kPa measurements for the same mixtures. Measurements in the air mixture and air + Ar show a large after-current caused by detached electrons. Through the addition of Ar, the displacement current increases. By contrast, in air + CO_2 mixture the after-current is reduced.

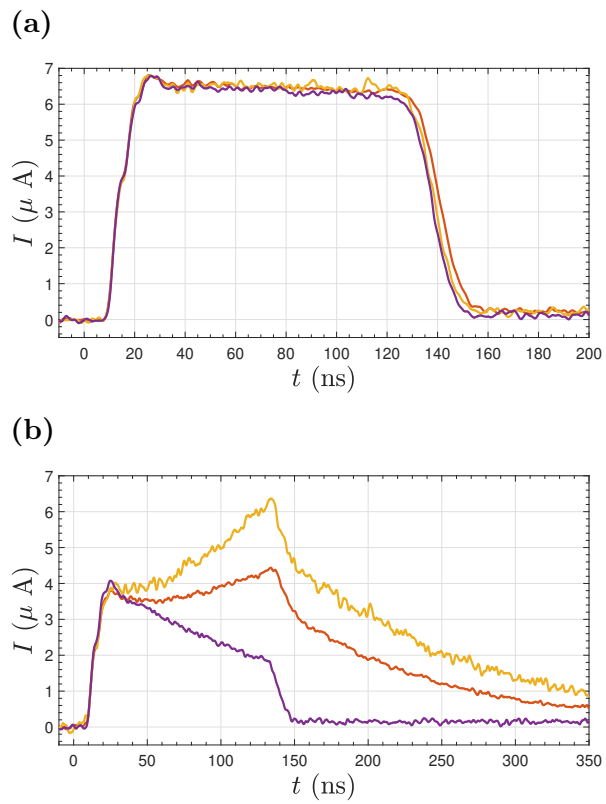

Figure 8: Different air like mixtures are color-coded:
(——) N_2-O_2-80-20%
(——) N_2-O_2-Ar-75-20-5%
(——) N_2-O_2-CO_2-75-20-5%
a) Displacement currents at 6 kPa at 15 mm electrode gap separation and E/N of 100 Td
b) Displacement currents at 60 kPa at 15 mm electrode gap separation and E/N of 99 Td

The effective ionization rate coefficient ν_{eff}/N for these air-like mixtures is shown in fig. 9. We compare the value of ν_{eff}/N obtained at low pressures (averaged ν_{eff}/N of measurements at 3 kPa to 8 kPa) to the value of ν_{eff}/N obtained at 60 kPa. The ν_{eff} are obtained by fitting the slope of the measured current, neglecting detachment. As the

electron drift velocity often cannot be detected, drift velocities from 3 kPa measurements are used to calculate α_{eff}. At low pressures, the ν_{eff}/N is similar for air and air + CO_2 but slightly higher for air + Ar. At 60 kPa, ν_{eff}/N of air and air + Ar shifts towards higher values. The value for air + CO_2 , on the other hand, remains similar to the low pressure values. For comparison, ${\nu_{\text{eff}}}^*/N$ of air 10 kPa evaluated more carefully in [14] and including ion and detachment processes is shown. The difference between ν_{eff}/N and ${\nu_{\text{eff}}}^*/N$ is largest below $(E/N)_{\text{crit}}$, for higher E/N values, the ${\nu_{\text{eff}}}^*/N$ converges towards $\nu_{\text{eff}}/N = \nu_{\text{i}}/N$-$\nu_{\text{a}}/N$. This finding might be specific to N_2-O_2 mixtures and different for other detaching gases. The resulting ${\nu_{\text{eff}}}^*/N$ at low pressures must still be affected by detachment but is probably due to the little number of ions or due the time scale not dominant in the obtained result.

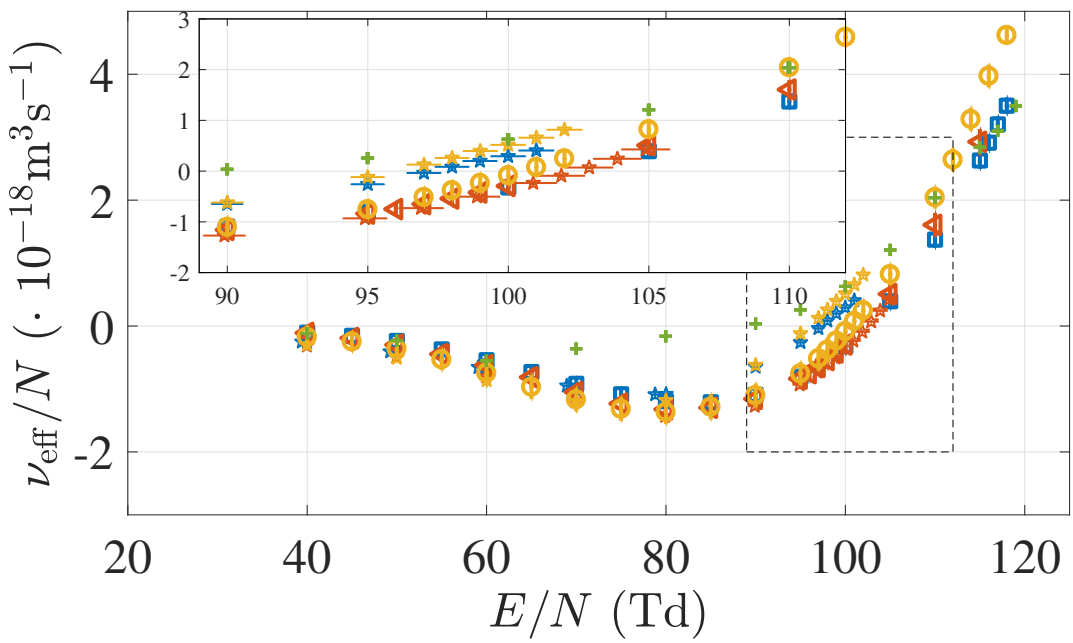

Figure 9: The effective ionization rate coefficient ν_{eff}/N for different air like mixtures, at different pressures. For different mixtures, pressures and methods different symbols and colors are used. Averaged low pressure measurements: (□) N_2-O_2-80-20%, (◁) N_2-O_2-CO_2-75-20-5%, (○) N_2-O_2-Ar-75-20-5%
(⋆) measurements at 60 kPa color of mixture remains
(+) N_2-O_2-80-20% at 10 kPa including ion kinetics and detachment [14]

Since air + CO_2 displacement currents show no after-current, an evaluation of electron and ion currents is possible using the model proposed in [13] as shown in fig. 10. The ion current model consists of one negative and one positive ion species. The fitted electron and ion current are in good agreement with the measurement.
The swarm parameters of N_2-O_2-CO_2-75-20-5% are shown in fig. 11 and 12. Through the additional information of the ion current, ν_{eff} could be separated in an attachment ν_{a} (plotted as negative rate) and ionization rate ν_{i} as depicted in fig. 11a. The longitudinal diffusion coefficient in fig. 11b increases with increasing E/N.

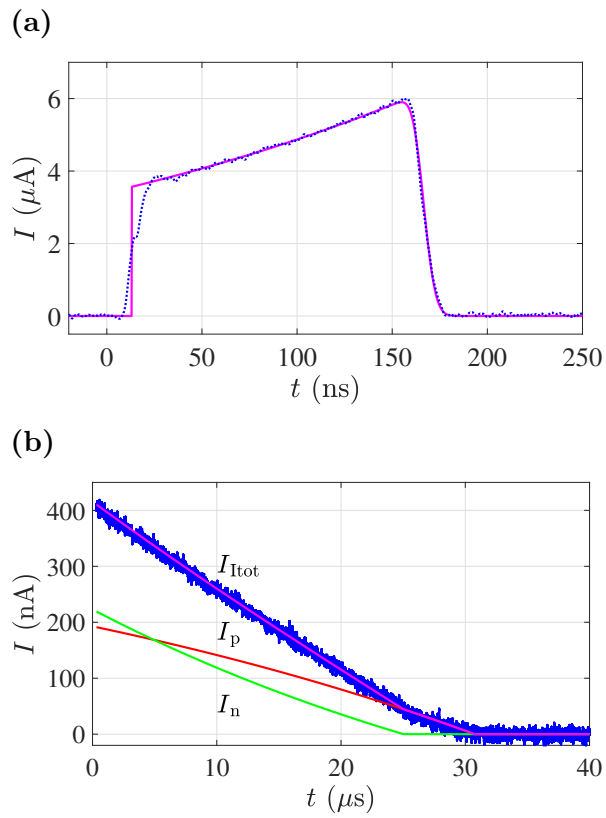

Figure 10: Measured current for N_2-O_2-CO_2-75-20-5% mixture at 60 kPa and electrode gap separation of 19 mm and E/N equal to 103 Td.
(——) measured displacement current
(——) fitted current
(——) fitted negative ion current
(——) fitted positive ion current
a) Measured time dependent electron current, ion current subtracted. **b)** Measured time dependent ion current current.

The electron and ion drift velocity w_e and w_i increase with increasing E/N as shown in fig. 12a and 12b. The velocity of negative ions is multiplied by (-1) for better visibility. Several positive and negative ion velocities from literature are included for comparison to our measurement data. The positive ion drift velocity of N_4^+ in N_2 [27] and O_2^+ in air [28] are similar and within our error bar of the measurement. Thus, these positive ions could not be distinguished by our measurement. CO_2^+ in CO_2 [29] and N_2^+ in N_2 [27, 29] have according to literature, a lower drift velocity. In [14], O_2^+ is assumed to be the dominant positive ion species in N_2-O_2 mixtures. Likewise, for negative ion drift velocities references for O_2^-, O_3^- and CO_3^- are in the same range within the error bar of the measurement and therefore the ions cannot be identified by their velocity. Even though several different positive and negative ion species may be present in the electrode gap due to similar drift velocities the simple model of one positive and one negative ion species is sufficient to describe the measured current.

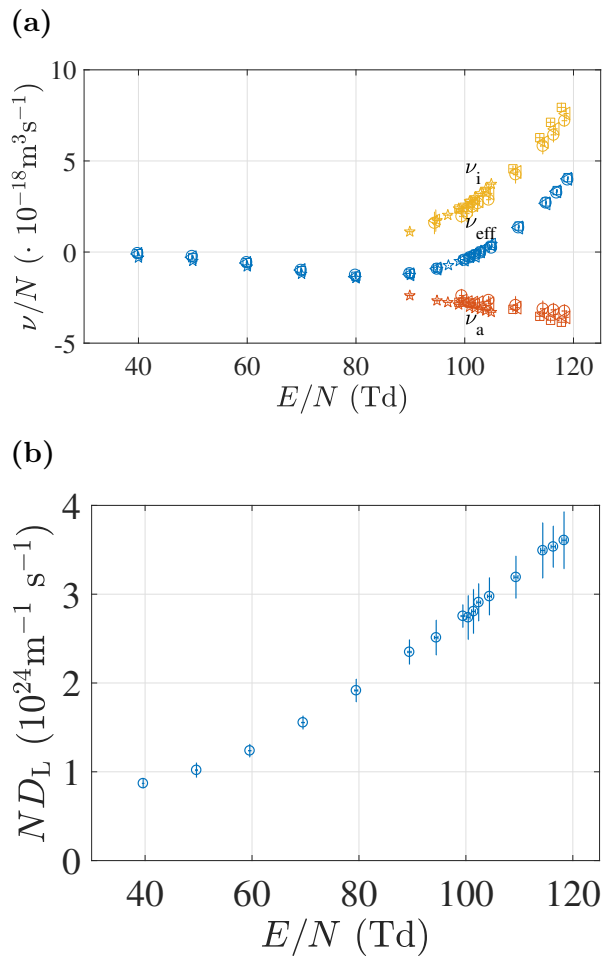

Figure 11: Different measured pressures (○) 3 kPa, (◁) 6 kPa, (□) 10 kPa, (⋆) 60 kPa in N_2-O_2-CO_2-75-20-5% **a)** Effective ionization rate coefficient ν_{eff}/N separated in ionization rate coefficient ν_{i}/N and attachment rate coefficient ν_{a}/N. **b)** Longitudinal diffusion coefficient ND_{L} for electrons.

4.5. Sensitivity of the streamer criterion to the streamer constant: example of air

The streamer criterion is used to connect the effective ionization coefficient to the breakdown voltage U_{Bd}. The streamer constant K used to fulfill the condition of breakdown is empirically determined. The air streamer constant K range spreads from 9.15 [15] up to 20 [30]. Previous K values around 20 were attributed to erroneous α_{eff} coefficients [15]. Nevertheless, K's influence on homogeneous electric field breakdowns in air is assumed to be small but still checked in fig. 13. In our case, the best agreement to reference data in several gases and mixtures (N_2 [31], CO_2 [31], air [31, 32, 33]) over a wide range of pd results when using K=12.

A difference in the value of K has a minor influence on the breakdown voltage as visible in fig. 13a. In absolute values, for $pd = 70$ bar mm, when K changes from 9.15 to 18, $U_{\text{Bd}}^{\text{calc}}$ changes from 185.8 to 191.4 kV. These values lie inside the calculated uncertainty of $U_{\text{Bd}}^{\text{calc}}$ when applying the measurement uncertainty in α_{eff} and K=12. In fact, the

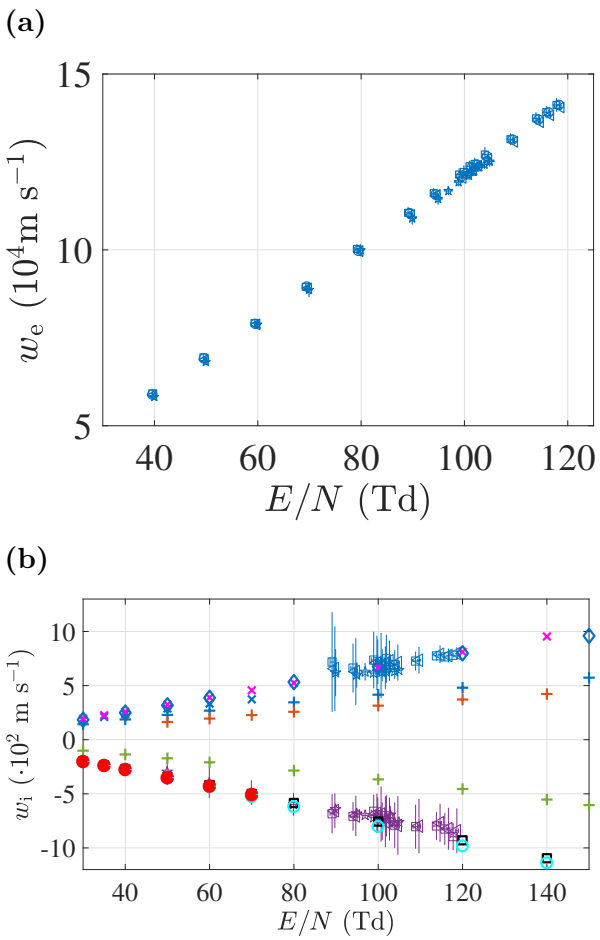

Figure 12: Different measured pressures (○) 3 kPa, (◁) 6 kPa, (□) 10 kPa, (⋆) 60 kPa in N_2-O_2-CO_2-75-20-5% **a)** Electron drift velocity w_e **b)** Ion drift velocity w_i of (——) positive ions with references (+) N_2^+ in N_2 Ellis [27], (x) N_2^+ in N_2 Viehland [29], (x) O_2^+ in air Viehland [28], (◇) N_4^+ in N_2 Ellis [27], (+) CO_2^+ in CO_2 Viehland [29] and (——) negative ions with references (+) CO_3^- in CO_2 Ellis [27], (□) O_2^- in air Viehland [28], (○) O_3^- in air Viehland [28], (●) CO_3^- in O_2 Viehland [28], the negative ion velocity is scaled by (-1).

$U_{\mathrm{Bd}}^{\mathrm{calc}}$ increases for increasing K. Even the reference data scatters in a similar range, which is better visible in fig. 13b. The streamer criterion is rather sensitive to deviations in the α_{eff}/N as the example of Bolsig+ shows. Our $U_{\mathrm{Bd}}^{\mathrm{calc}}$ from swarm data best matches the $U_{\mathrm{Bd}}^{\mathrm{meas}}$ reference measurements from the IEC-60052 standard [33].

4.6. Breakdown measurements and Paschen Law

The reproducibility of the breakdown measurements is high as fig. 14 shows; the different colors and symbols indicate one measurement series each. For N_2 and O_2, the maximum scatter in the median values of different measurement series is 0.8 kV at measured voltages above 120 kV. Besides the small possible $U_{\mathrm{Bd}}^{\mathrm{meas}}$ maxima for certain mixtures

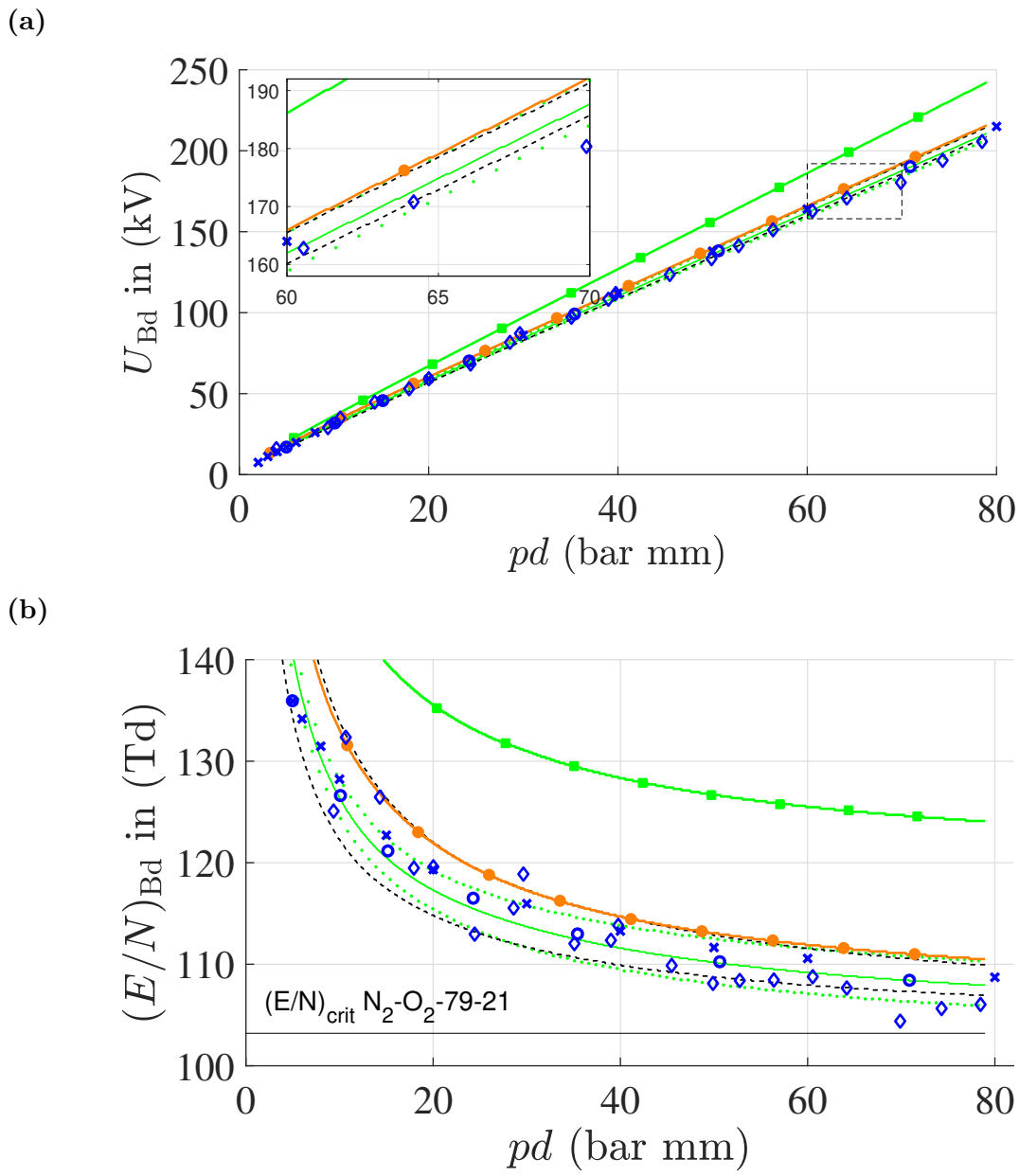

Figure 13: Sensitivity of calculated $U_{\mathrm{Bd}}^{\mathrm{calc}}$ and $(E/N)_{\mathrm{Bd}}^{\mathrm{calc}}$ to changes in the streamer constant K using measured α_{eff} [16] and comparison to measured $U_{\mathrm{Bd}}^{\mathrm{meas}}$ reference data of air.

(——) N_2-O_2-79-21, K=12, (·····) calculated uncertainty of U_{Bd} and $(E/N)_{\mathrm{Bd}}$, K =12, (- - - -) N_2-O_2-79-21, K=9.15, 18, (–●–) N_2-O_2-79-21 Magboltz, (–■–) N_2-O_2-79-21 Bolsig+, (○) IEC-60052 [33], (x) Dakine 1974 [32], (◇) Gruenberg 1978 [31]

a) Breakdown voltage U_{Bd}.

b) Density-reduced breakdown field $(E/N)_{\mathrm{Bd}}$.

the majority of measured mixtures have a $U_{\mathrm{Bd}}^{\mathrm{meas}}$ voltage between the pure gases. Example measurements for pure gases are shown as their scatter is representative for all measured mixtures. Although all measurements have similar experimental conditions,

the scatter of the 16 and 84 percentiles shown in fig.14, increases for O_2 (approx. 5 kV) and CO_2 (approx. 10 kV) compared to N_2 (approx. 1 kV). The default number of shots for one measurements series is set to 250. As a consequence of problems with electromagnetic compatibility and electrode conditioning effect some measurement series at higher *pd* show a reduced number of measurements.

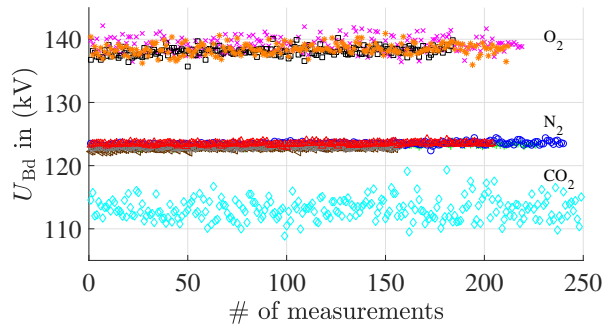

Figure 14: Breakdown voltage measurement series. Several series of 250 individual breakdowns at 50 bar mm, normalized electrode separation of 15 mm and temperature of 293 K for pure N_2, CO_2 and O_2.

In homogeneous electric fields, U_{Bd} should only depend on *pd*, the product of pressure and electrode separation distance (Paschen law). To test the setup and the Paschen law, breakdown series at different distance *d* but same *pd* were conducted in N_2-O_2 80-20 % and are shown in fig. 15. For a *d* of 10 up to 20 mm at $pd = 25$ bar mm the measured $U_{\mathrm{Bd}}^{\mathrm{meas}}$ were similar and scattered within the normal range of the error bar.

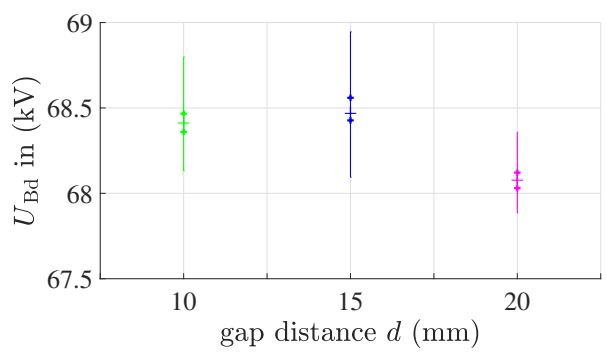

Figure 15: Breakdown measurements at different electrode separation d = 10, 15 and 20 mm for the same $pd = 25$ bar mm in N_2-O_2 80-20 %

4.7. Comparison of breakdown measurements to calculated breakdown voltages using the streamer criterion with measured swarm data

To calculate the streamer criterion for N_2-O_2 mixtures, the α_{eff} from [16] averaged at low pressure was used. In fig. 16, the calculated $U_{\mathrm{Bd}}^{\mathrm{calc}}$ and measured $U_{\mathrm{Bd}}^{\mathrm{meas}}$ breakdown voltages of N_2-O_2 mixtures are shown. Not every mixture presented in the figure is

measured with both experiments, therefore an acronym PT for pulsed Townsend experiment and Bd for breakdown was used. The agreement between $U_{\mathrm{Bd}}^{\mathrm{calc}}$ derived by the streamer criterion and measured $U_{\mathrm{Bd}}^{\mathrm{meas}}$ is very good. As fig. 16 shows, trends and nearly the absolute value of the two different applied methods agree. Mixtures with an O_2 concentration higher than 40% have a similar breakdown voltage as pure O_2. Swarm experiments indicate slightly higher $U_{\mathrm{Bd}}^{\mathrm{calc}}$ as pure O_2 for mixtures above an O_2 concentration of 60%. In fig. 16b) it can be seen that the different $(E/N)_{\mathrm{Bd}}^{\mathrm{calc}}$ lines for mixtures cross around 30 bar mm, which means that at low pd values mixtures with O_2 concentrations <10 % are best and at high pd values those with an O_2 content $\geq 40\,\%$. This may lead to confusing results as sometimes in publications different experimental settings (different d at the same p) are compared.

For N_2-CO_2 mixtures, the comparison of the streamer criterion $U_{\mathrm{Bd}}^{\mathrm{calc}}$ and measured $U_{\mathrm{Bd}}^{\mathrm{meas}}$ breakdown voltages is shown in fig. 17. The highest breakdown voltage $U_{\mathrm{Bd}}^{\mathrm{calc}}$ obtained from swarm data is that of pure N_2, whereas breakdown data suggests that a mixture of N_2-CO_2 80-20% has a slightly higher median value. Apart from that, CO_2 breakdown measurements show a significantly higher scatter which increases the median value, compared to measurements with a lower scatter like pure N_2. The $(E/N)_{\mathrm{Bd}}^{\mathrm{calc}}$ lines for different N_2-CO_2 mixtures probably cross above pd values of 80 bar mm. The absolute difference in calculated $U_{\mathrm{Bd}}^{\mathrm{calc}}$ and measured $U_{\mathrm{Bd}}^{\mathrm{meas}}$ is small as shown in fig. 16a. The good agreement of both methods is emphasized on the example of CO_2 at 70 bar mm where the difference for them in $(E/N)_{\mathrm{Bd}}^{\mathrm{calc}}$ and $(E/N)_{\mathrm{Bd}}^{\mathrm{meas}}$ is 2-3 Td with an absolute $(E/N)_{\mathrm{Bd}}^{\mathrm{calc}}$ value around 85 Td.
In fig. 18, measured $U_{\mathrm{Bd}}^{\mathrm{meas}}$ and calculated $U_{\mathrm{Bd}}^{\mathrm{calc}}$ breakdown voltages of CO_2-O_2 mixtures are presented. Mixtures with a concentration of 50% O_2 and higher are already in the range of the breakdown voltage of pure O_2. The admixture of 5% CO_2 slightly increase the electric strength of pure O_2 by 1-2% whereas a concentration of 20% CO_2 is again below the breakdown voltage of pure O_2 in the measured range.
As shown in section 4.4, detachment and conversion processes affect O_2 mixtures, if the negative ions are not stabilized. The influence of the pressure dependence on the streamer criterion in air, air + Ar and air + CO_2 is shown in fig. 19. Results from averaged low pressure α_{eff} indicate that for high pd values, the admixture of Ar leads to a lower breakdown strength, which is confirmed by the breakdown measurements. On the contrary, calculated results from low pressures show a slightly higher breakdown strength for air than air + CO_2 which contradicts with the findings from the breakdown results. As stated in section 4.4, $U_{\mathrm{Bd}}^{\mathrm{calc}}$ calculated from regular derived α_{eff} [13] overestimates the breakdown voltage whereas α_{eff} from low pressure including ion kinetics [14] measurements underestimates the calculated $U_{\mathrm{Bd}}^{\mathrm{calc}}$. Using α_{eff} derived from 60 kPa swarm measurements for air and air + Ar the calculated $U_{\mathrm{Bd}}^{\mathrm{calc}}$ decreases and fits the breakdown results better. Due to the problems of measuring swarm data (possible space charge effects or even breakdowns) at these elevated pressures and E/N above $(E/N)_{\mathrm{crit}}$, the x-axis of fig. 19b was extended to 150 bar mm to include calculated $U_{\mathrm{Bd}}^{\mathrm{calc}}$ of

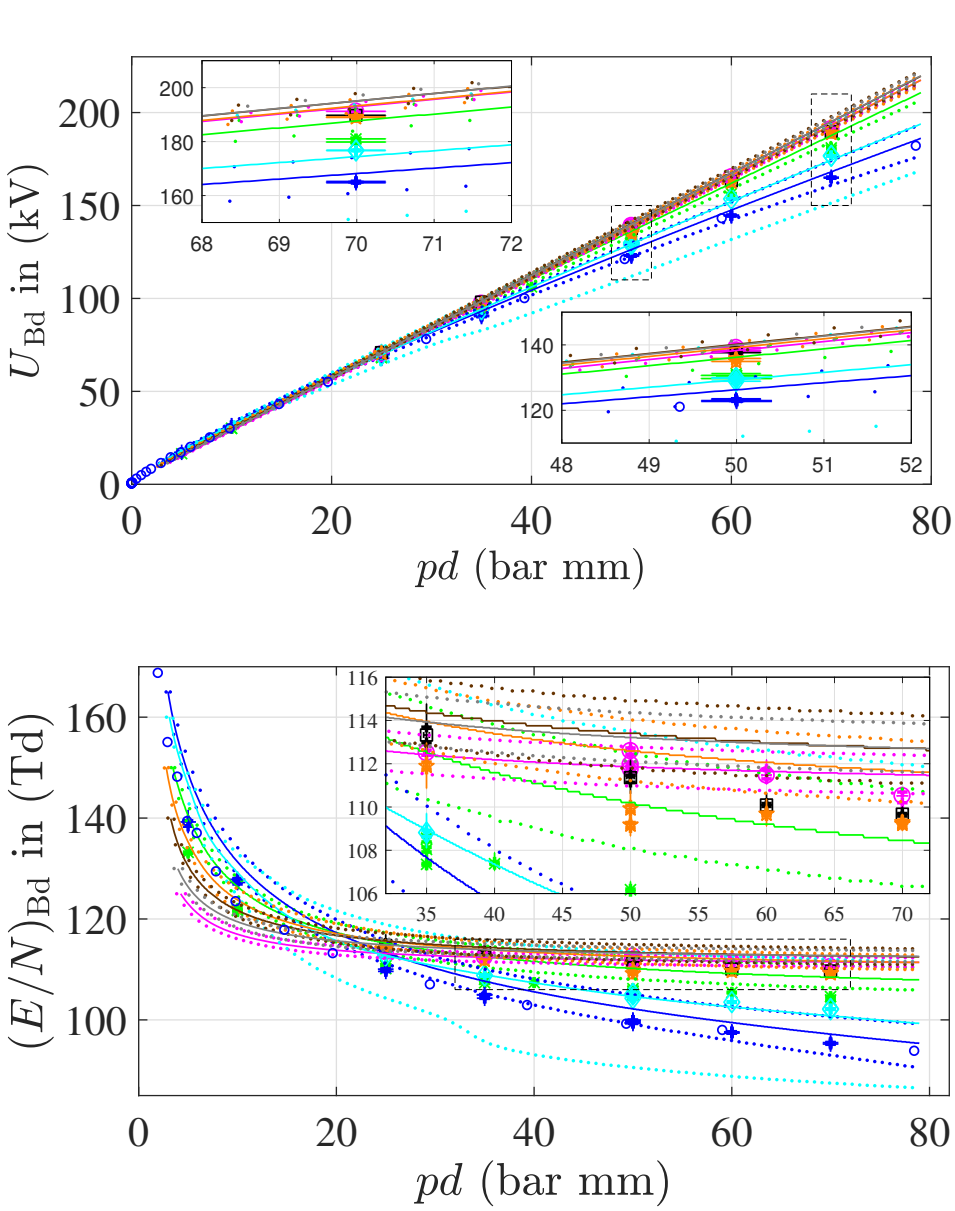

Figure 16: Comparison of U_{Bd} calculated by the streamer criterion $U_{\mathrm{Bd}}^{\mathrm{calc}}$ (lines) to measured $U_{\mathrm{Bd}}^{\mathrm{meas}}$ in breakdown experiments (symbols) for different N_2-O_2 mixtures which are color-coded. The error in α_{eff}/N leads to an error in the calculated $U_{\mathrm{Bd}}^{\mathrm{calc}}$ which is shown by the dotted lines. Reference is (○) the measured U_{Bd} for N_2 from Dakin 1974 [31].
(——) PT; (+) Bd; for N_2-100% (——) PT; (○) Bd; for O_2-100% (◇) Bd for N_2-O_2-90-10% (——) PT; for N_2-O_2-92-8% (——) PT; for N_2-O_2-79-21% (x) Bd; for N_2-O_2-80-20% (□) Bd; for N_2-O_2-50-50% (——) PT; (⋆) Bd; for N_2-O_2-60-40% (——) PT; for N_2-O_2-40-60% (——) PT; for N_2-O_2-20-80%
a) Breakdown voltage. U_{Bd} **b)** Density-reduced electric breakdown field $(E/N)_{\mathrm{Bd}}$, T=293 K.

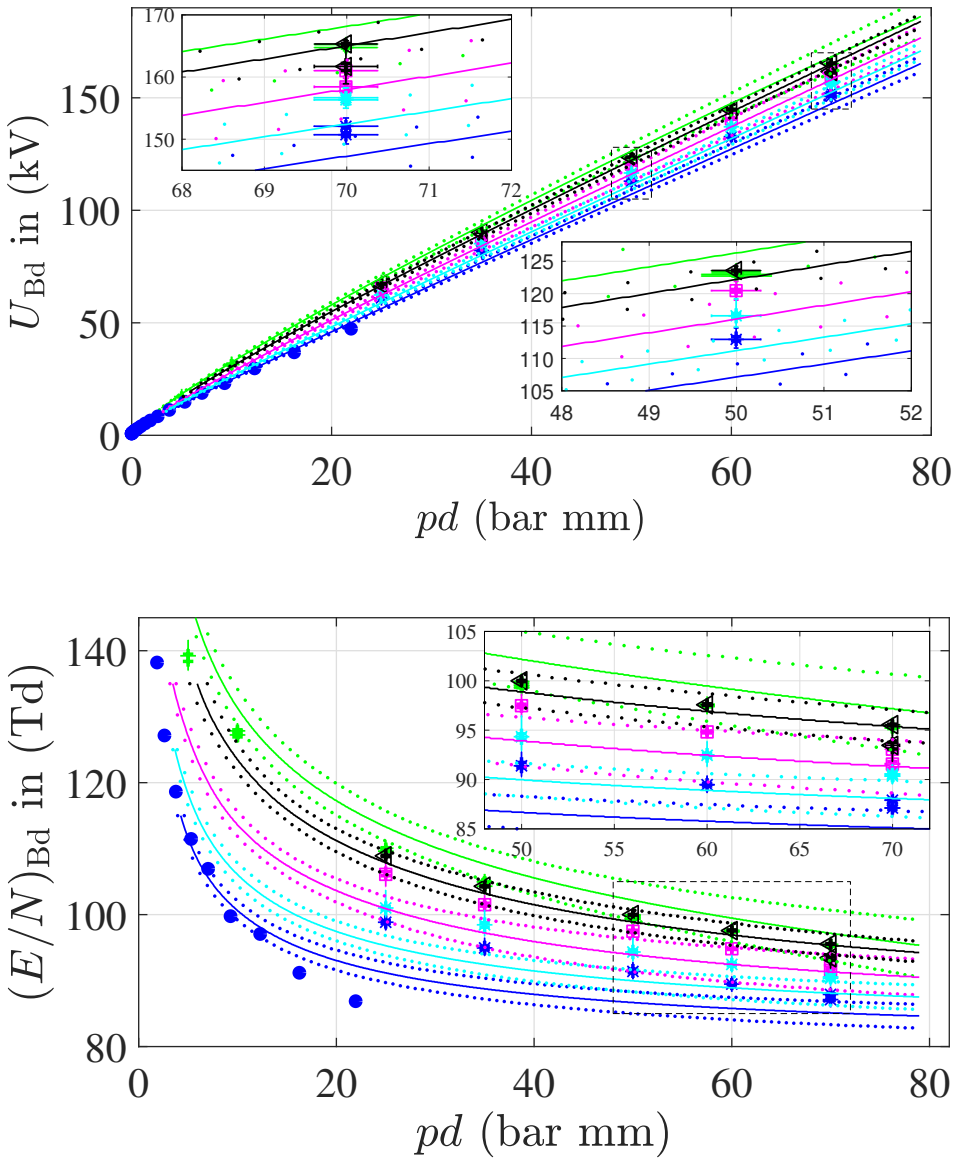

Figure 17: Comparison of U_{Bd} calculated $U_{\mathrm{Bd}}^{\mathrm{calc}}$ (lines) to measured $U_{\mathrm{Bd}}^{\mathrm{meas}}$ (symbols) for different N_2-CO_2 mixtures which are color-coded. The error in α_{eff}/N leads to an error in the calculated $U_{\mathrm{Bd}}^{\mathrm{calc}}$ which is shown by the dotted lines. (•) measured $U_{\mathrm{Bd}}^{\mathrm{meas}}$ in CO_2 from Dakin 1974 [31].
(——) PT; (+) Bd; for N_2-100% (——) PT; (*) Bd; for CO_2-100% (——) PT; (◁) Bd; for N_2-CO_2-80-20% (——) PT; (□) Bd; for N_2-CO_2-50-50% (——) PT; (*) Bd; for N_2-CO_2-20-80%
a) Breakdown voltage U_{Bd}. **b)** Density-reduced electric breakdown field $(E/N)_{\mathrm{Bd}}$, T=293 K.

air and air + CO_2, which could only be measured up to a very limited E/N value above $(E/N)_{\mathrm{crit}}$. Low and high pressure calculations for air + CO_2 show no pressure

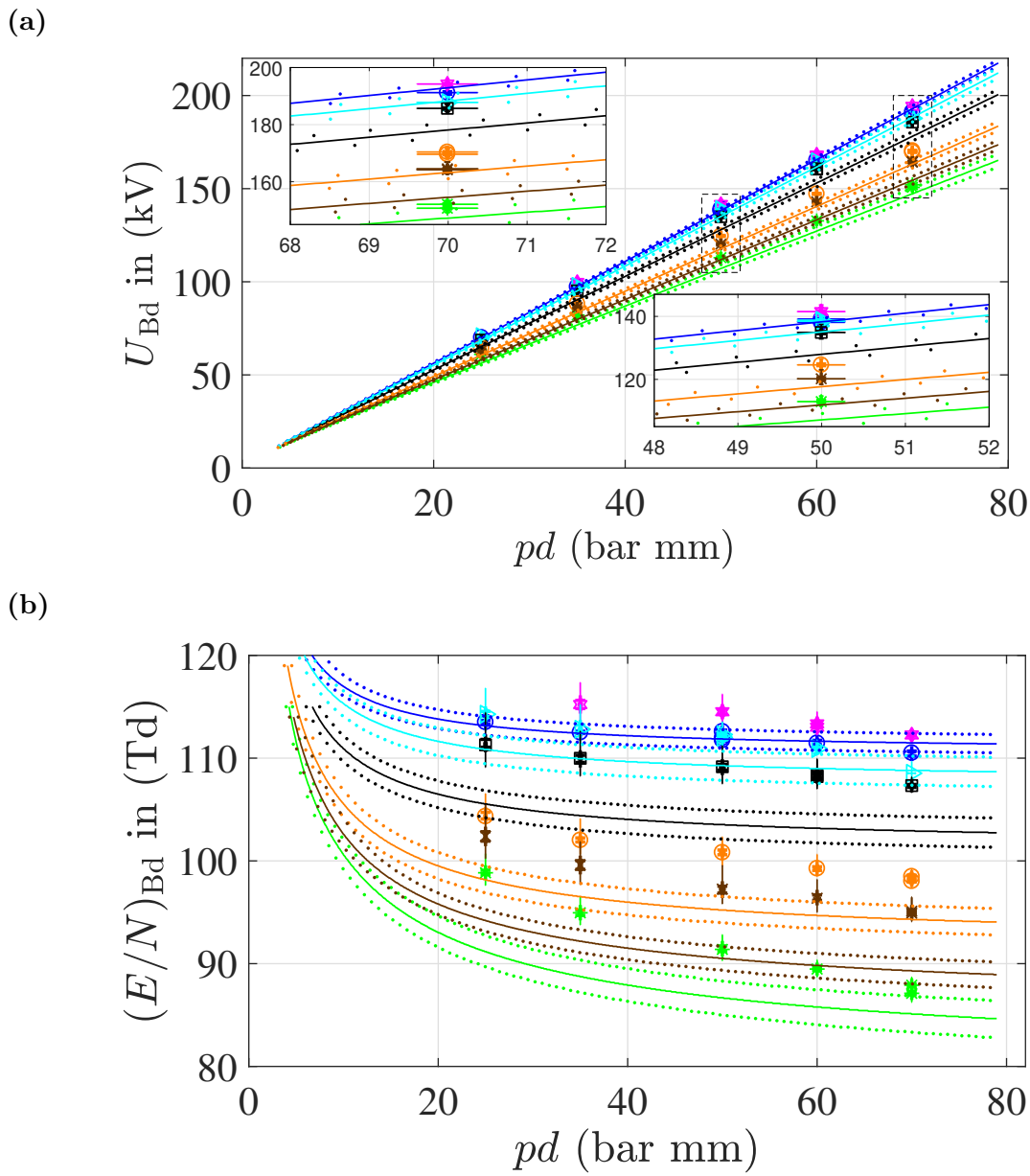

Figure 18: Comparison of U_{Bd} calculated $U_{\mathrm{Bd}}^{\mathrm{calc}}$ by the streamer criterion (lines) to measured $U_{\mathrm{Bd}}^{\mathrm{meas}}$ in breakdown experiments (symbols) for different CO_2-O_2 mixtures which are color-coded. The error in α_{eff}/N leads to an error in the calculated $U_{\mathrm{Bd}}^{\mathrm{calc}}$ which is shown by the dotted lines.
(——) PT; (*) Bd; for CO_2-100% (——) PT; (○) Bd; for O_2-100% (——) PT; for CO_2-O_2-92-8% (x) Bd; for CO_2-O_2-90-10% (——) PT; (○) Bd; for CO_2-O_2-80-20% (——) PT; (□) Bd; for CO_2-O_2-50-50% (——) PT; (▷) Bd; for CO_2-O_2-20-80% (——) PT; (⋆) Bd; for CO_2-O_2-5-95% Bd
a) Breakdown voltage U_{Bd}. **b)** Density-reduced electric breakdown field $(E/N)_{\mathrm{Bd}}$, T=293 K.

dependence. Calculated $U_{\mathrm{Bd}}^{\mathrm{calc}}$ from higher pressures agree better to measured $U_{\mathrm{Bd}}^{\mathrm{meas}}$, this is most clear in the case of air + Ar as visible in fig. 19. In fig. 19a the added references from Imamovic 2011 [34] seem to agree for air + Ar whereas measurements of air deviate.

5. Discussion and Conclusion

The discussion is structured as follows: first, the different mixtures are compared looking only at one method and second the different results from different methods are compared. The methods according to section 3 are, a) using $(E/N)_{\mathrm{crit}}$, b) using the streamer criterion to calculate $U_{\mathrm{Bd}}^{\mathrm{calc}}$ and c) $U_{\mathrm{Bd}}^{\mathrm{meas}}$ from direct breakdowns.

5.1. $(E/N)_{crit}$ of binary mixtures

The highest $(E/N)_{\mathrm{crit}}$ is measured in N_2-O_2 mixtures or pure O_2. A small CO_2 admixture around 5% to O_2 was not measured with the swarm experiment but it might have the highest $(E/N)_{\mathrm{crit}}$ according to breakdown measurements.

5.2. Swarm data of N_2-O_2 mixtures and admixtures of Ar and CO_2

Displacement currents in air, air + CO_2 and air + Ar result in similar displacement currents at low pressures as seen in fig. 9. The currents show significant differences for higher pressures as shown on the example of 60 kPa measurements. Swarm measurements at higher pressures like 60 kPa are therefore of interest. In the best case, the obtained α_{eff} can be used for estimations of even higher pressures applied in gas insulated equipment for high voltage. In the air + CO_2 mixture the addition of CO_2 presumably stabilizes the unstable O^- ion [7] to CO_3^- in a three-body process eq. (9). Although, an N^2 dependence was not found in our measurements.

$$\mathrm{O}^- + \mathrm{CO}_2 + M \rightarrow \mathrm{CO}_3^{-*} + M \rightarrow \mathrm{CO}_3^- + M \tag{9}$$

5.3. U_{Bd} of different mixtures comparing measured and calculated results

In fig. 20, mixtures with highest U_{Bd} are compared to O_2 and air. Above 45 bar mm, O_2 mixtures show clearly a higher U_{Bd} as mixtures without O_2. In this *pd* range and above, calculated $U_{\mathrm{Bd}}^{\mathrm{calc}}$ and measured $U_{\mathrm{Bd}}^{\mathrm{meas}}$ for pure O_2 show a very good agreement, whereas at 70 bar mm, the measured breakdown voltage decreases compared to calculated. The decrease of $U_{\mathrm{Bd}}^{\mathrm{meas}}$ is attributed to electromagnetic compatibility problems in breakdown measurements at high *pd*. Due to the electromagnetic pulses caused by the breakdowns, the number of recorded breakdowns is lower than the default 250 breakdowns of one measurement series. They might be slightly affected by the initial conditioning process.

By comparing the calculated $U_{\mathrm{Bd}}^{\mathrm{calc}}$ and measured $U_{\mathrm{Bd}}^{\mathrm{meas}}$, two main effects at *pd* higher than 40 bar mm were found. First, a small admixture of around 5% CO_2 to a N_2-O_2 mixture could increase the breakdown voltage by 1 to 2%. Second, in this *pd* range,

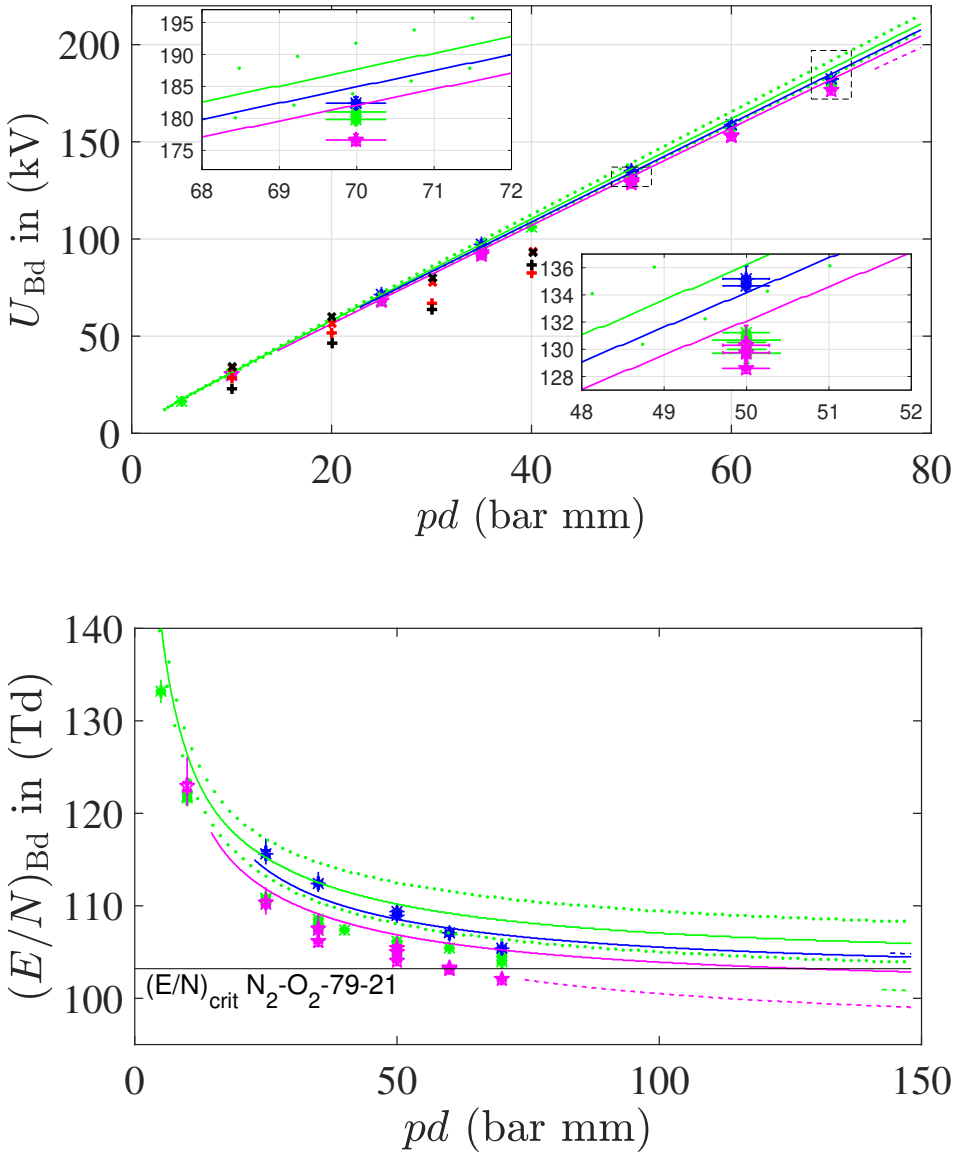

Figure 19: Comparison of U_{Bd} calculated by the streamer criterion $U_{\mathrm{Bd}}^{\mathrm{calc}}$ (lines) to measured $U_{\mathrm{Bd}}^{\mathrm{meas}}$ in breakdown experiments (symbols) for different air like mixtures which are color-coded. The error in α_{eff}/N leads to an error in the calculated $U_{\mathrm{Bd}}^{\mathrm{calc}}$ which is shown by the dotted lines. Dashed lines are swarm measurements at 60 kPa.
(——) PT; (x) Bd; for N_2-O_2-80-20% (——) PT; (*) Bd; for N_2-O_2-CO_2-75-20-5% (——) PT; (⋆) Bd; for N_2-O_2-Ar-75-20-5%
a) Breakdown voltage U_{Bd}. References Imamovic 2011 [34] for homogeneous DC field breakdown sphere-sphere arrangement for (+) N_2-O_2-80-20% and (x) N_2-O_2-Ar-75-20-5% black positive polarity and red negative polarity **b)** Density-reduced electric breakdown field $(E/N)_{\mathrm{Bd}}$, T =293 K.

calculated $U_{\mathrm{Bd}}^{\mathrm{calc}}$ from N_2-O_2 mixtures with 60 and 80% O_2 concentration show a slightly

(a)

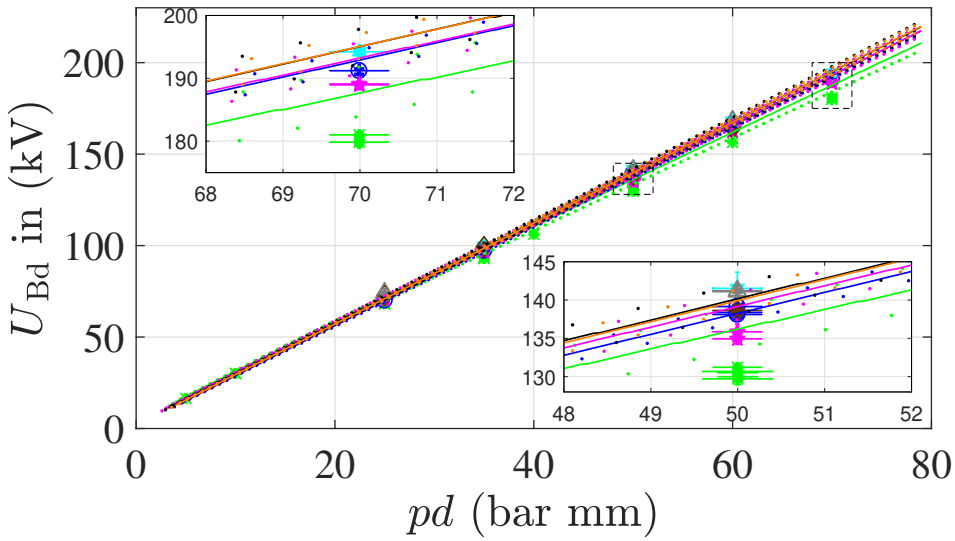

(b)

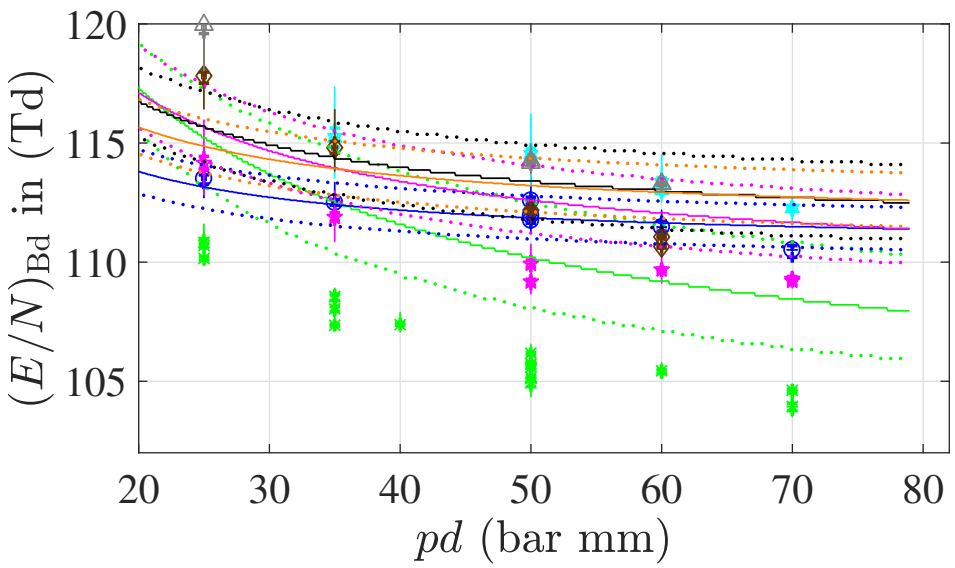

Figure 20: Comparison of U_{Bd} calculated $U_{\mathrm{Bd}}^{\mathrm{calc}}$ (lines) to $U_{\mathrm{Bd}}^{\mathrm{meas}}$ measured in breakdown experiments (symbols) for most interesting mixtures which are compared to air. The different mixtures are color-coded. The error in α_{eff}/N leads to an error in the calculated $U_{\mathrm{Bd}}^{\mathrm{calc}}$ which is shown by the dotted lines.
(x) Bd; for N_2-O_2-80-20% (——) PT; for N_2-O_2-79-21% (——) PT; (○) Bd; for O_2-100% (——) PT; (⋆) Bd; for N_2-O_2-60-40% (——) PT; (⋆) Bd; for CO_2-O_2-5-95% (——) PT; for N_2-O_2-40-60% (——) PT; for N_2-O_2-20-80% (◇) Bd; for N_2-O_2-CO_2-55-40-5% (△) Bd; for N_2-O_2-CO_2-35-60-5%
a) Breakdown voltage U_{Bd}. **b)** Density-reduced electric breakdown field $(E/N)_{\mathrm{Bd}}$, $\mathrm{T} = 293\,\mathrm{K}$.

increased U_{Bd} compared to O_2. The improvement of these mixtures compared to air is around 3% based on calculated $U_{\mathrm{Bd}}^{\mathrm{calc}}$ and 8% for measured $U_{\mathrm{Bd}}^{\mathrm{meas}}$. Based on these results, $U_{\mathrm{Bd}}^{\mathrm{meas}}$ of two ternary mixtures were measured and are shown in fig. 20. The mixture N_2-O_2-CO_2 with 40% O_2 and 5% CO_2 content has a breakdown strength close to pure O_2 but a significant reduced O_2 content compared to pure O_2. Compared to air, the measured breakdown strength is improved by 6%. The other mixture is N_2-O_2-CO_2 with 60% O_2 and 5% CO_2 content, it has the highest possible $U_{\mathrm{Bd}}^{\mathrm{meas}}$ for atmospheric gas mixtures. Compared to air, the measured breakdown strength is improved by 8%.

5.4. Comparison of $(E/N)_{crit}$ and $(E/N)_{\mathrm{Bd}}$ or U_{crit} and U_{Bd}

For non attaching gases or mixtures with a very low attachment rate, $(E/N)_{\mathrm{crit}}$ is not a useful criterion to determine the electric strength of a gas. This is due to the absence of a zero crossing of α_{eff} and the slow increase of α_{eff}. In the case of N_2 and N_2-CO_2 mixtures with low CO_2 concentration only looking at $(E/N)_{\mathrm{crit}}$, underestimates the electric strength of $N_2$and these mixtures. In breakdown measurements of N_2 and N_2-CO_2 mixtures, $U_{\mathrm{Bd}}^{\mathrm{meas}}$ decreases with increasing CO_2 concentration in contrast to estimations from $(E/N)_{\mathrm{crit}}$ in the measured *pd* range. For N_2-CO_2 mixtures with low CO_2 concentration the bias on α_{eff} from PT measurements dominates calculated $U_{\mathrm{Bd}}^{\mathrm{calc}}$ and it reduces $U_{\mathrm{Bd}}^{\mathrm{calc}}$ in the *pd* range above 150-180 bar mm.

The example of air in fig. 8b shows that low pressure measurements and the resulting α_{eff} used to calculate $(E/N)_{\mathrm{crit}}$ and $U_{\mathrm{Bd}}^{\mathrm{calc}}$, might not cover all effects present in the gas sample to fit the displacement current correctly. Ideally, the model should capture all relevant electron, ion and detachment processes as presented in [14]. In fig. 19, $U_{\mathrm{Bd}}^{\mathrm{calc}}$ calculated from low pressure α_{eff} are compared to results measured at high pressures. Measured and calculated U_{Bd} from low pressure measurements agreed better for the air + CO_2 mixture with less detachment. Low pressure results for air and air + Ar overestimated $U_{\mathrm{Bd}}^{\mathrm{calc}}$ compared to measured $U_{\mathrm{Bd}}^{\mathrm{meas}}$. High pressure α_{eff} (60 kPa in the example) agreed better to measured $U_{\mathrm{Bd}}^{\mathrm{meas}}$ for air and air + Ar in the *pd* range around 60 to 80 bar mm. According to [14] in N_2-O_2 mixtures the pressure dependent ${\nu_{\mathrm{eff}}}^*/N$ converges towards $\nu_{\mathrm{eff}}/N = \nu_{\mathrm{i}}/N$-$\nu_{\mathrm{a}}/N$ for increasing pressures and E/N values. As shown in fig.9, in the $(E/N)_{\mathrm{Bd}}^{\mathrm{calc}}$ range for air from 108 to 120 Td the difference of the methods [13] and [14] was only small. Therefore, we conclude that calculated $U_{\mathrm{Bd}}^{\mathrm{calc}}$ from low pressure measurements are sufficient accurate.
Besides comparing the different methods to obtain U_{Bd} within the *pd* range where direct breakdown measurements were possible with the presented setup, the *pd* range above is of particular interest for the calculated $U_{\mathrm{Bd}}^{\mathrm{calc}}$. In table 2, the two possible ways to calculate U_{Bd} ($(E/N)_{\mathrm{crit}}$ and streamer criterion) are compared to $U_{\mathrm{Bd}}^{\mathrm{meas}}$ from the IEC standard [33] at $pd = 152$ bar mm. A *pd* of 152 bar mm corresponds to a p around 1 MPa at a $d = 15$ mm. The *pd* values above 150 bar mm might be of interest for practical applications. Again, very good agreement was achieved between both

	U_{Bd} in (kV)
$U_{\mathrm{Bd}}^{\mathrm{meas}}$ IEC	390
$U_{\mathrm{Bd}}^{\mathrm{calc}}$ α_{eff} @ low pressure	397
$U_{\mathrm{Bd}}^{\mathrm{calc}}$ α_{eff} @ 60 kPa	378
U_{crit} from $(E/N)_{\mathrm{crit}}$ (102.9 Td)	386
CO_2 $U_{\mathrm{Bd}}^{\mathrm{calc}}$ @ low pressure	311
CO_2 U_{crit} from $(E/N)_{\mathrm{crit}}$ (80.4 Td)	302

Table 2: Air and CO_2breakdown voltage calculated using $(E/N)_{\mathrm{crit}}$ and the streamer criterion. Air is compared to the IEC Standard at pd=152 bar mm.

calculated $U_{\mathrm{Bd}}^{\mathrm{calc}}$ and $U_{\mathrm{Bd}}^{\mathrm{meas}}$ of the IEC standard. Hence, we conclude that the applied methods using PT results give accurate results and can be used at high pd values at pd > 100 bar mm where the value of $(E/N)_{\mathrm{Bd}}$ approaches $(E/N)_{\mathrm{crit}}$. Industry is interested in CO_2, as a gas used in switching applications. At $pd = 152$ bar mm the U_{Bd} of CO_2 is around 78 % of U_{Bd}in air.
Pressure dependent ${\nu_{\mathrm{eff}}}^*/N$ and $(E/N)_{\mathrm{crit}}$ in fig. 9 seem to be a contradiction to measurements of a single $U_{\mathrm{Bd}}^{\mathrm{meas}}$ in fig. 15 for different sets of p and d at a constant pd. The measured $U_{\mathrm{Bd}}^{\mathrm{meas}}$ at 25 bar mm air, leads to a $(E/N)_{\mathrm{Bd}}^{\mathrm{meas}}$ of 115 Td. At this E/N, far above $(E/N)_{\mathrm{crit}}$, the different methods [12] and [13] give the same results. However, when $(E/N)_{\mathrm{Bd}}$ is around $(E/N)_{\mathrm{crit}}$ the different methods start to deviate. To achieve this condition in breakdown experiments, measurements at least at $pd = 80$ bar mm or higher and low pressures (around 10 k) must be performed. Ideally, pressures starting from 10 k up to 200 kPa or higher should be measured. The resulting conditions for breakdown experiments are rather difficult to achieve in real system. The pressures 10 k and 200 kPa would lead to electrode gap distances of 800 mm and 40 mm.

5.5. Summary and conclusion

Overall, it was shown that the breakdown voltage in homogeneous fields can be reliably predicted by applying the streamer criterion and using α_{eff} values measured in PT experiments. Three different methods to obtain U_{Bd} were shown, a) calculated via $(E/N)_{\mathrm{crit}}$, b) calculated with the streamer criterion (both a) and b) using α_{eff} from a pulsed Townsend experiment) and c) via direct breakdown voltage measurements. The example of air shows that above 100 bar mm $U_{\mathrm{Bd}}^{\mathrm{calc}}$ obtained by the streamer criterion converges to U_{crit} calculated via $(E/N)_{\mathrm{crit}}$. The applied methods found optimal mixtures in N_2-O_2 and CO_2-O_2 with a N_2 content between 20-40% and a CO_2 concentration of around 5%. In general the admixture of 5% CO_2 improved U_{Bd} of O_2 mixtures around 2%. Based on previous findings, ternary mixtures (40% to 80% O_2, 5% CO_2 and N_2) were investigated. Compared to air the breakdown voltage increased for about 8%. When applying method a) and b) the input parameter α_{eff} could show pressure dependence through detachment and ion conversion processes. However, in O_2 mixtures, the model

neglecting additional detachment and ion conversion processes, still leads to accurate calculated $U_{\mathrm{Bd}}^{\mathrm{calc}}$ values. Since for different mixtures U_{Bd} increases with pd in different slopes, the optimal mixture depends on the application. For real application, mixtures of atmospheric gases will have to be applied at pressures above today used values of 0.5 M to 0.6 MPa to keep dimensions reasonable. This is possible as the boiling point is very low. At these high pressures we propose that N_2-O_2-CO_2 mixtures are best with the mixing ratio of 55-40-5% or 35-60-5%.

Acknowledgments

This work is financially supported by GE Grid (Switzerland) GmbH, Pfiffner Technologie AG, ABB Switzerland Ltd and Siemens AG.

[1] T Stocker et al, editor. *Anthropogenic and Natural Radiative Forcing*. Cambridge University Press, Cambridge, United Kingdom and New York, NY, USA, 2013.

[2] L Niemeyer. A systematic search for insulation gases and their environmental evaluation. In *Gaseous Dielectrics VIII*, pages 459–464. Springer, 1998.

[3] M Rabie and C Franck. Computational screening of new high voltage insulation gases with low global warming potential. *IEEE Transactions on Dielectrics and Electrical Insulation*, 22(1):296–302, 2015.

[4] Y Kieffel. Characteristics of g3 -an alternative to SF_6. In *Dielectrics (ICD), 2016 IEEE International Conference on*, volume 2, pages 880–884. IEEE, 2016.

[5] J Mantilla, N Gariboldi, S Grob, and M Claessens. Investigation of the insulation performance of a new gas mixture with extremely low GWP. In *Electrical Insulation Conference (EIC), 2014*, pages 469–473. IEEE, 2014.

[6] T a Rokunohe et al. Development of 72-kv high-pressure air-insulated gis with vacuum circuit breaker. *Electrical engineering in Japan*, 157(4):13–23, 2006.

[7] J Moruzzi and D Price. Ionization, attachment and detachment in air and air-CO_2 mixtures. *Journal of Physics D: Applied Physics*, 7(10):1434, 1974.

[8] T Rokunohe et al. Fundamental insulation characteristics of air; N_2, CO_2, N_2/O_2, and SF_6/N_2 mixed gases. *Electrical Engineering in Japan*, 155(3):9–17, 2006.

[9] A Winter et al. Solid/ gaseous insulation systems for compact HVDC solution. In *Cigre, Paris*, 2014. Paper D1-102.

[10] Dominik A Dahl, Timm H Teich, and Christian M Franck. Obtaining precise electron swarm parameters from a pulsed townsend setup. *Journal of Physics D: Applied Physics*, 45(48):485201, 2012.

[11] P Haefliger and Franck C M. Detailed precision and accuracy analysis of swarm parameters from a pulsed townsend experiment. *Review of Scientific instruments*, 89(2):023114, 2018.

[12] A Hoesl, P Haefliger, and C M Franck. Measurement of ionization, attachment, detachment and charge transfer rate coefficients in dry air around the critical electric field. *Journal of Physics D: Applied Physics*, 50(48):485207, 2017.

[13] A Chachereau, M Rabie, and CM Franck. Electron swarm parameters of the hydrofluoroolefine HFO1234ze. *Plasma Sources Science and Technology*, 25(4):045005, 2016.

[14] P Haefliger, A Hoesl, and CM Franck. Measurement of rate coefficients for electron and ion processes in pure oxygen and $\mathrm{N_2 - O_2}$ mixtures. *Journal of Physics D: Applied Physics*, submitted.

[15] K Petcharaks. *Applicability of the streamer breakdown to inhomogeneous gas gaps*. PhD thesis, ETH, Diss. no. 11192, 1995.

[16] P Haefliger and Franck C M. Critical electric field strength and effective ionization coefficient

measurements of nitrogen-oxygen mixtures with variable mixing ratio. In *Cigre, Paris*, 2014. Paper D1-307.

[17] W Hauschild and W Mosch. *Statistical techniques for high-voltage engineering.* IET, 1992.

[18] Hanspeter Schmid and Alex Huber. Measuring a small number of samples, and the 3σ fallacy: Shedding light on confidence and error intervals. *IEEE Solid-State Circuits Magazine*, 6(2):52–58, 2014.

[19] P Haefliger and Franck C M. Swarm parameter measurements of argon / oxygen mixtures. In *Posmol, Kanazawa*, 2014.

[20] M Yousfi et al. Electron swarm coefficients in CO_2-N_2 and CO_2-O_2 mixtures. *IEEE Transactions on Plasma Science*, 37(6):764–772, 2009.

[21] L Frommhold. Über verzögerte Elektronen in Elektronenlawinen, insbesondere in Sauerstoff und Luft, durch Bildung und Zerfall negativer Ionen (O^-). *Fortschritte der Physik*, 12(11):597–642, 1964.

[22] H F A Verhaart and P C T Van der Laan. The influence of water vapor on avalanches in air. *Journal of applied physics*, 55(9):3286–3292, 1984.

[23] ETHZ database. Lxcat. `https://fr.lxcat.net/home/`. Accessed: 2017-02-21.

[24] S F Biagi. Monte carlo simulation of electron drift and diffusion in counting gases under the influence of electric and magnetic fields. *Nuclear Instruments and Methods in Physics Research Section A: Accelerators, Spectrometers, Detectors and Associated Equipment*, 421(1):234–240, 1999.

[25] GJM Hagelaar and LC Pitchford. Solving the boltzmann equation to obtain electron transport coefficients and rate coefficients for fluid models. *Plasma Sources Science and Technology*, 14(4):722, 2005.

[26] LXCat Database. Lxcat. `https://fr.lxcat.net/home/`. Accessed: 2017-02-21.

[27] HW Ellis, RY Pai, EW McDaniel, EA Mason, and LA Viehland. Transport properties of gaseous ions over a wide energy range. *Atomic Data and Nuclear Data Tables*, 17(3):177–210, 1976.

[28] C Viehland, Land Kirkpatrick. Relating ion/neutral reaction rate coefficients and cross-sections by accessing a database for ion transport properties. *International journal of mass spectrometry and ion processes*, 149:555–571, 1995.

[29] LA Viehland and EA Mason. Transport properties of gaseous ions over a wide energy range, iv. *Atomic Data and Nuclear Data Tables*, 60(1):37–95, 1995.

[30] H Raether. *Electron avalanches and breakdown in gases.* Butterworths, 1964.

[31] John M Meek and John Drummond Craggs. *Electrical breakdown of gases.* John Wiley & Sons, 1978.

[32] T Dakin. Breakdown of gases in uniform fields-paschen curve for nitrogen, air, and sulfur hexafluoride. *Electra*, 32:61–82, 1974.

[33] IEC. Voltage measurement by means of standard air gaps. IEC 60052, 2002.

[34] D Imamovic. *Umweltfreundliche Isoliergase fuer gasisolierte Leitungen zur Hochspannungs-Gleichstrom-Uebertragung.* PhD thesis, TU Graz, 2011.